

Dynamically Tunable Fano Metamaterials through the Coupling of Graphene Grating and Square Closed Ring Resonator

Jun Ding¹ · Bayaner Arigong¹ · Han Ren¹ · Jin Shao¹ · Mi Zhou¹ · Yuankun Lin^{1,2} · Hualiang Zhang¹

Received: 9 March 2015 / Accepted: 8 June 2015 / Published online: 18 June 2015
© Springer Science+Business Media New York 2015

Abstract We present the numerical studies of a novel hybrid graphene-metal Fano metamaterial, which is composed of a graphene grating (graphene ribbon array) and a square closed ring resonator (SCRR) separated by a dielectric substrate. The destructive interference between the narrow and broad electrical dipolar surface plasmons induced respectively on the surface of the graphene ribbon and the SCRR leads to the classical analog of electromagnetically induced transparency (EIT). By decreasing the thickness of the substrate spacer (enhancing the coupling between the two components), a double EIT system could be achieved. More importantly, the transparency windows in the hybrid structures can be actively controlled by varying the applied gate voltage on the graphene ribbon. Large effective group index and small loss within the transparency windows suggest the promising slow-light applications.

Keywords Graphene · Tunable · Fano metamaterial · Electromagnetically induced transparency

Introduction

The electromagnetically induced transparency (EIT) is a quantum effect that could give rise to a sharp peak

within a broad transmittance dip in the transmission spectrum, resulting in a narrow and asymmetric Fano lineshape [1]. This plasmonic EIT phenomenon, featuring sharp resonance and steep dispersion, has been widely utilized in the applications of plasmonic switchers [2], plasmonic rulers [3], slow light [4], bio-sensors [5], etc. Generally, the analog to EIT could be explained either as the result of engaging “trapped mode” resonances [6] or by the destructive interference between a radiative bright mode and a less-radiative dark mode [7, 8]. Different types of mode or resonance can be induced in a metallic subwavelength structure due to either localized surface plasmon polaritons (SPPs) or propagating SPPs, which are collective oscillations of electrons at a metal-dielectric interface [9]. EIT and EIT-like phenomenon could then be achieved by manipulating the coupling or hybridization of these SPPs. Despite enormous research interest of EIT based on metallic metamaterials (MTMs), the performance of the SPPs in metals is greatly limited because of the difficulty or impossibility in dynamically controlling the properties of metals and the existence of large material losses in the terahertz and far infrared frequency (THz/far-IR) ranges. Thus, most of the observed EIT effects based on MTMs have been working at fixed frequencies, which means the EIT resonances have to be tuned to work at different frequencies by varying the physical structure parameters. However, it is difficult if not impossible to change the geometrical parameters of the structure after fabrication. Therefore, the active manipulation over the subwavelength constitutive elements of the plasmonic EIT system is of great importance.

Many approaches to achieve dynamic tuning of the EIT have emerged by integrating MTMs with optically active materials, such as nonlinear media [10], liquid crystals [11],

✉ Jun Ding
stevendingjun@gmail.com

✉ Hualiang Zhang
hualiang.zhang@unt.edu

¹ Department of Electrical Engineering, University of North Texas, 3940 N. Elm St., Denton, TX 76207, USA

² Department of Physics, University of North Texas, Denton, TX 76207, USA

phase-change materials [12], etc. Especially graphene [13], a single layer of carbon atoms gathered in a honeycomb lattice, has attracted tremendous interest due to its unique optical and electrical properties, such as ultra-high electron mobility, gate-tunable carrier densities, and ability to support SPPs [14–16]. Graphene manifests strong absorption of light in the near-infrared and visible range [17]. At lower frequencies such as THz/far-IR range, the intraband transition of electrons dominates, and graphene behaves like metals but with stronger SPP confinement to the surface and relatively lower loss. Graphene appears to be a good candidate for designing and engineering tunable devices because its conductivity can be controlled by shifting the Fermi energy levels, which may be potentially tuned from -1 to 1 eV by chemical doping [18] or electrical gating [19]. So far, graphene has been extensively studied for applications in photonics and optoelectronics [20, 21], plasmonic metamaterials [22, 23], and medical sciences [24].

In this paper, we proposed a highly wavelength-tunable EIT metamaterial structure composed of a graphene grating and a gold square closed ring resonator (SCRR) separated by a SiO_2 substrate working at THz/far-IR range. Graphene grating with low loss works as a “quasi-dark” mode with high Q-factor [25, 26], while the gold SCRR works as a “bright” mode with low Q-factor [27]. The destructive interferences between them could result in EIT and generate transmitting spectra with Fano-like profiles. Interestingly, when the coupling between the graphene grating and SCRR is increased by gradually decreasing the thickness of the substrate, an extra transmission peak gradually becomes evident; thus, a double EIT-like system could be realized. The single EIT and double EIT resonances are further studied by analyzing the field distributions. More importantly, the active control of the EIT resonances is demonstrated by varying the Fermi energy of the graphene grating without changing any physical structures. The transparency window could be further manipulated by changing the width of the graphene ribbon and the surrounding medium as well. Large group index and small loss could be achieved with the proposed structures, which suggest potential applications in slow-wave devices.

Design and Simulation of the Proposed Fano Metamaterial

Figure 1a schematically depicts an array of the proposed structure, which consists of an array of gold SCRR, a SiO_2 substrate spacer, and a layer of graphene grating (i.e., graphene ribbon array). The graphene grating is along the y -direction, and the SCRR is right beneath (along the positive z -direction) the graphene ribbon. The graphene layer, the substrate, and the gold SCRR are illustrated in blue, pink, and yellow, respectively. Figure 1b displays the bottom view of a unit cell of the proposed structure with the detailed geometrical parameters.

The periodicity P of the unit cell is identical in both x - and y -direction and fixed at $6 \mu\text{m}$, and the line width of the SCRR is fixed at 100 nm . The width of the graphene ribbon, the length of the SCRR, and the thickness of the SiO_2 substrate are denoted as W , L , and t_{sub} , respectively, which play important roles in the resonances of the hybrid structure.

The dielectric constant of the SiO_2 substrate is taken as 3.9, and the permittivity of gold is described by the Drude model with the plasma frequency $\omega_p = 1.37 \times 10^{16} \text{ s}^{-1}$ and the damping constant $\omega_c = 4.08 \times 10^{13} \text{ s}^{-1}$ [28]. In our simulations, the graphene sheet is treated as an ultrathin film with a thickness of t . The well-known Kubo formula [29] is used for deriving the surface conductivity of the graphene sheet $\sigma_g = \sigma^{\text{intra}} + \sigma^{\text{inter}}$ including the intraband and interband transition contributions. In the THz/far-IR range, i.e., $\mu_c \gg \hbar\omega \gg k_B T$, the intraband transition contribution dominates [30] and the surface conductivity simplifies to a Drude-like expression

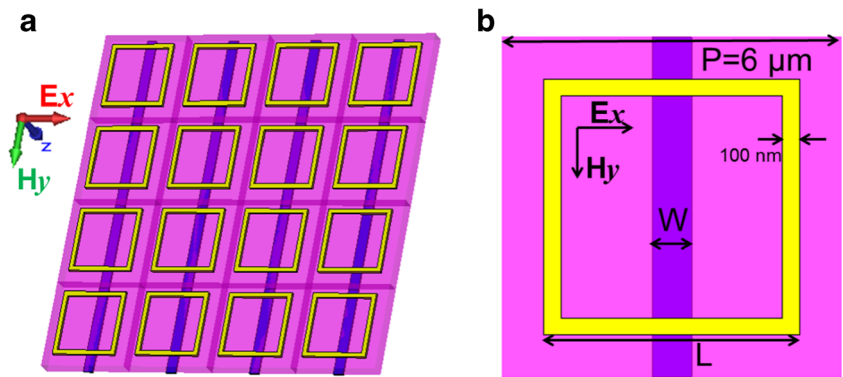
$$\sigma_g(\omega, \mu_c) = \frac{e^2 \mu_c}{\pi \hbar^2} \frac{i}{\omega + i \tau^{-1}} \quad (1)$$

where e is the electron charge, μ_c is the Fermi energy level of the graphene ribbon, \hbar is the reduced Planck constant, and the carrier relaxation time is τ taking into account impurity, defect, and electron-phonon scattering process, which is assigned as $\tau = 1 \text{ ps}$ at a room temperature in the simulations. As can be seen from Eq. (1), changing the Fermi energy μ_c allows one to change the propagation characteristics of graphene plasmons. Then, the dielectric constant of graphene can be obtained by $\varepsilon = 1 + \frac{j\sigma_g}{\varepsilon_0 \omega t}$, where $t = 1 \text{ nm}$ is a typical value of the thickness of graphene in modeling and simulation [31].

Results and Analysis of the Proposed Fano Metamaterial

A plane wave of TM polarization (its magnetic field is perpendicular to the x - z plane) impinges normally along the $+z$ -direction from the bottom of the structure. When excited by this incident wave separately, the electrical dipolar SPPs can be induced both on the SCRR and the graphene ribbon. Figure 2a, b shows the transmission spectra for the SCRR only with different L and graphene grating only with different W , respectively. (In these simulations, we fix the $\mu_c = 0.7 \text{ eV}$ for graphene grating, and $t_{\text{sub}} = 0.8 \mu\text{m}$ for the dielectric substrate). Note that the dipolar SPPs induced on graphene grating and the SCRR have narrow (high Q-factor) [25, 26] and broad (low Q-factor) [27] resonant spectral responses, respectively. Thus, the graphene grating and the SCRR can be deemed as the “quasi-dark” mode and the “bright” mode in the classical analog of EIT, respectively. It is pointed out in [32] that the EIT could be generated if the two electrical dipolar SPP structures have close or identical resonances with different Q-

Fig. 1 **a** Schematic of the array of the proposed hybrid structure; **b** a unit cell of the proposed structure



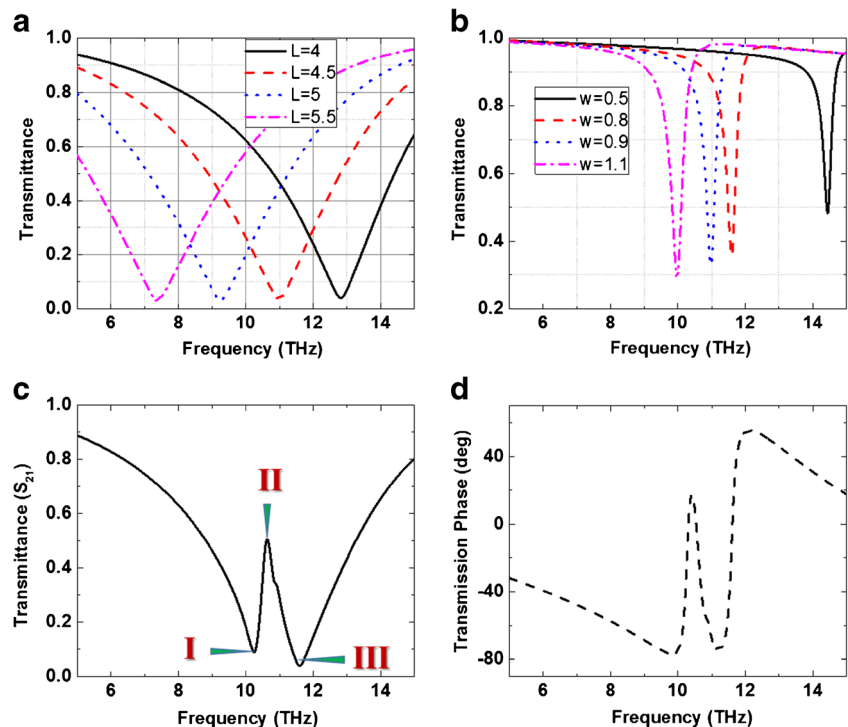
factors. As can be seen from Fig. 2a, b, the SCRR with $L=4.5 \mu\text{m}$ and graphene grating with $W=0.9 \mu\text{m}$ have almost the same resonant frequency at around 11 THz and are chosen as an example, which by no means is the limitation of the proposed structure. As expected, the Fano lineshape and a narrow EIT window are demonstrated in Fig. 2c. The corresponding transmission phase is illustrated in Fig. 2d, which reflects the abrupt phase change.

Figure 3a, b demonstrates the characteristic snapshots of current density at the surfaces of SCRR and graphene ribbon at frequencies I (10.55 THz), II (11.08 THz), and III (11.86 THz) in Fig. 2c, respectively. Note that the maximum current amplitudes in Fig. 3a, b are 1×10^{12} and 8×10^{10} , respectively. It can be observed that the current strength in the radiative component (SCRR) is much larger than that in less-radiative component (graphene ribbon) at all three frequencies (I, II, and III). However, at the peak of transmission window

(II), the current in SCRR is suppressed while relative stronger surface current is induced in the graphene ribbon, compared to the ones induced at I and III. Furthermore, it is noted that the currents (as marked by the black arrows) in the SCRR and graphene ribbon flow out of phase in x -direction at I but in phase at frequency III. This current distribution results in the corresponding near field x -component electric field E_x ($0.1 \mu\text{m}$ underneath SCRR in x - y plane) presented in Fig. 3c. As can be seen from Fig. 3c, at the transmission dips (I and III), the graphene ribbon and the SCRR have very strong couplings, while the two components have very weak coupling at II. Thus, the single EIT-like effect could be the result of the destructive interference between the strongly induced graphene ribbon and the suppressed SCRR.

In order to better understand how the coupling between the two components changes the transparency window, we conduct the parametrical study by varying the thickness of the

Fig. 2 **a** Transmittance of the SCRR only for different L ; **b** transmittance of the graphene grating only for different W ; **c, d** transmittance and transmission phase of the hybrid structure, with $L=4.5 \mu\text{m}$ and $W=0.9 \mu\text{m}$



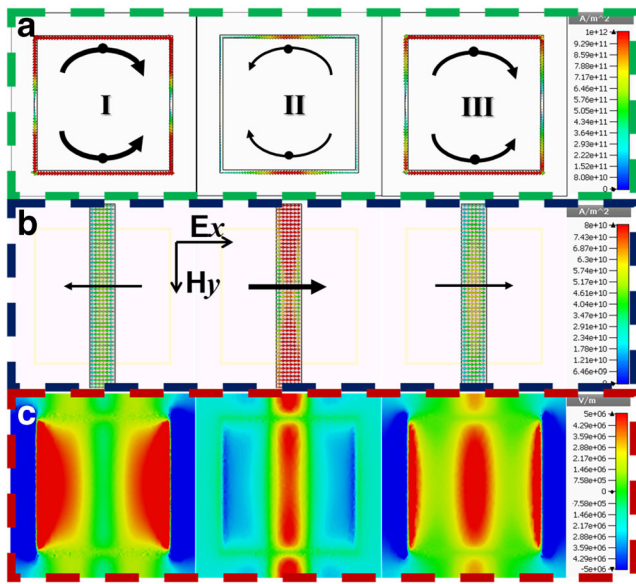


Fig. 3 a The current density at the surface of SCRR; b the current density at the surface of graphene ribbon; c the near field of E_x in x - y plane $0.1 \mu\text{m}$ underneath the SCRR at the three labeled frequencies (I~III) labeled in Fig. 2(c), respectively. (The widths of the arrow show the relative strength of the current density in (a) and (b): wider line indicates stronger strength)

substrate t_{sub} . Figure 4a displays the transmittances for different t_{sub} . As the thickness decreases from 3 to $1 \mu\text{m}$, indicating the enhancement of the coupling between the two individual

components, a transparency window between two transmission dips gradually becomes prominent. More interestingly, when the thickness decreases further, another transmission dip gradually emerges, which leads to a double EIT-like system using the same structure. The characteristic snapshots of current density at the surfaces of SCRR and graphene ribbon at five labeled frequencies in Fig. 4a are displayed in Fig. 4b and Fig. 4c, respectively. And E_x distributions for the five frequencies are plotted in Fig. 4d. It is noted that the maximum magnitude I_1 in Fig. 4c is 20 times smaller than I_0 (the maximum magnitude in Fig. 4b). As can be seen from Fig. 4b, c, although much more complicated surface currents are induced at the surfaces of SCRR and graphene ribbon at frequencies II, III, and IV, there still exist certain similarities between the current distributions at frequencies I and V and the current distributions at frequencies I and III in Fig. 3a, b. Once again, we observe that the currents are suppressed in SCRR, and relatively strong currents are induced in graphene ribbon at the peaks of the transmission windows (II and IV). In addition, as can be seen from Fig. 4d, the couplings between these two constituting components are very weak at frequencies II and IV and strong at transmission dips (frequencies I, III, and IV). Except for the much more complicated surface current and E_x distributions, the coupling mechanism of the double EIT-like system is similar to that of the aforementioned single EIT-like system.

Fig. 4 a Transmittances of the hybrid structures for different t_{sub} ; b the current density at the surface of SCRR; c the current density at the surface of graphene ribbon; d the near field of E_x in x - y plane $0.1 \mu\text{m}$ underneath the SCRR at the five labeled frequencies (I~V in Fig. 4(a)), respectively

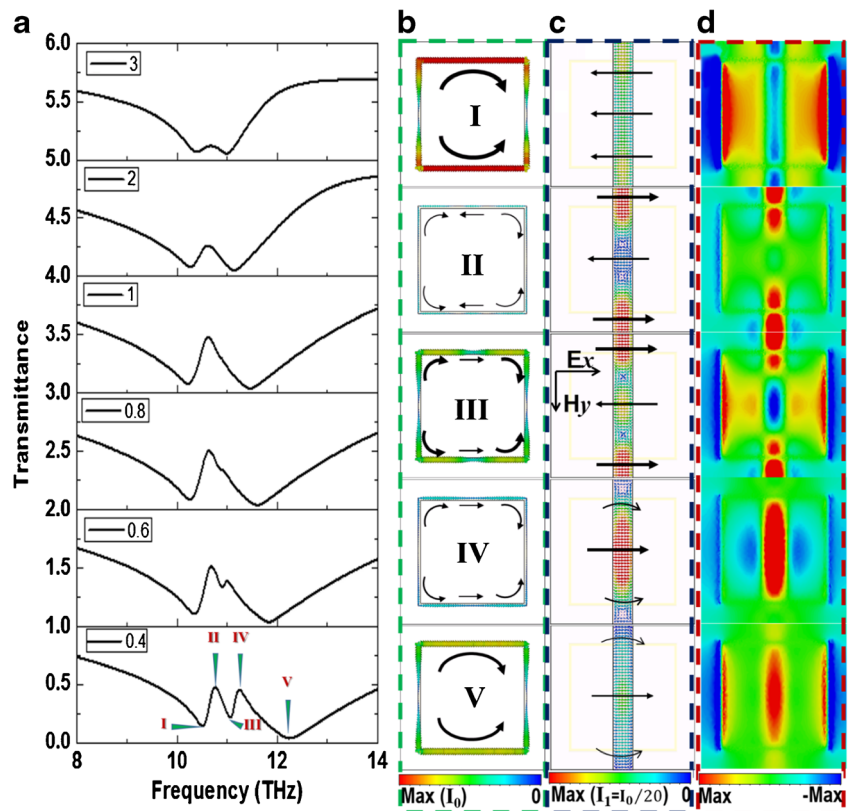
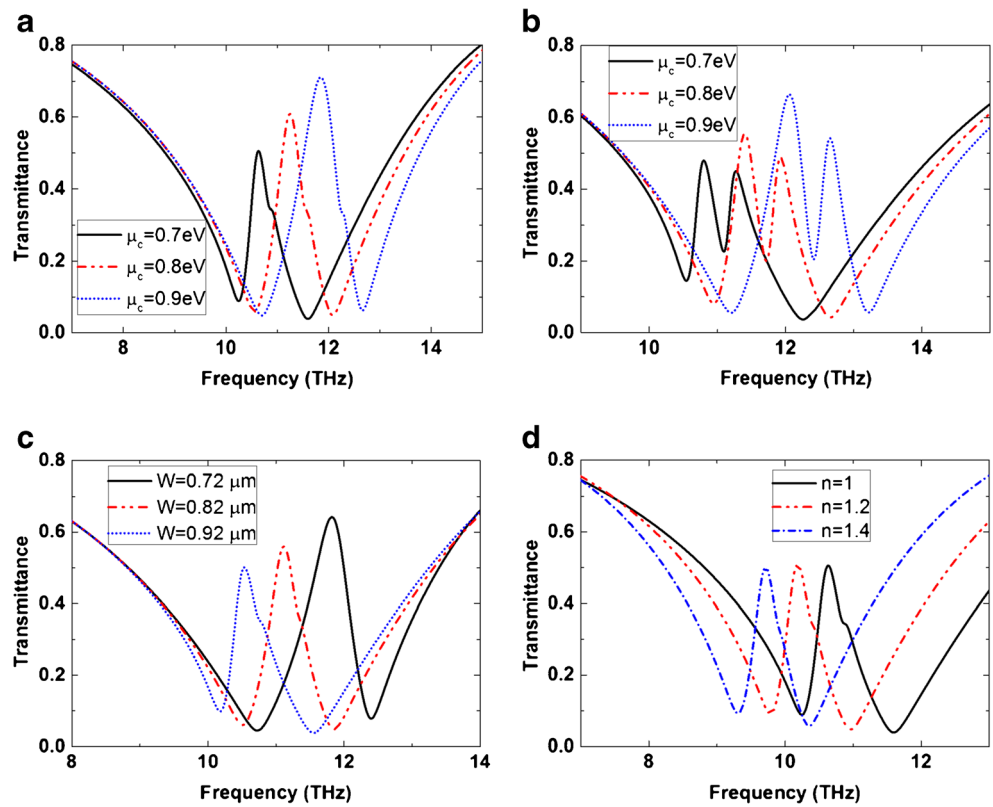


Fig. 5 **a, b** Transmittance for the hybrid structure with various Fermi energy μ_c for $t_{\text{sub}}=0.8 \mu\text{m}$ and $t_{\text{sub}}=0.4 \mu\text{m}$, respectively ($W=0.9 \mu\text{m}$); **c** transmittance for the hybrid structure with various width of the graphene ribbon ($t_{\text{sub}}=0.8 \mu\text{m}$, $\mu_c=0.7 \text{ eV}$); **d** transmittance for the hybrid structure with various background refractive index n ($t_{\text{sub}}=0.8 \mu\text{m}$, $\mu_c=0.7 \text{ eV}$ and $W=0.9 \mu\text{m}$)

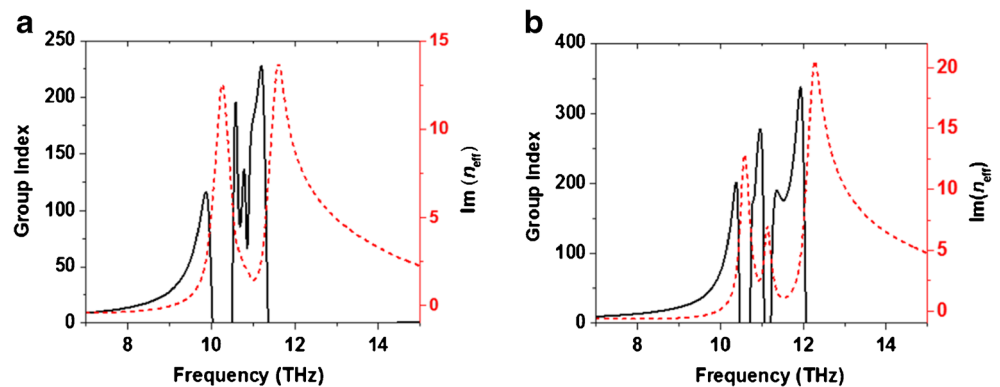


Tunability and Slow Wave Characteristic of the Proposed Fano Metamaterial

Next, we study the tunability of the Fano resonance in the designed hybrid structures. One of the major advantages of the graphene-based structure compared with the noble metal-based structures is the active tunability, which can be achieved by electrostatic gating. Specifically, the optical response of the designed structures can be changed by applying different bias voltages so that they can work at different wavelengths (frequencies) without re-optimizing or reconstructing the

physical structure. This is highly desirable in many practical applications since it is very difficult to change the physical structure after fabrication. We first study the effect of applying different Fermi energy levels on the responses of the hybrid structures. Figure 5a, b shows the transmittances for $t_{\text{sub}}=0.8 \mu\text{m}$ (single Fano resonance) and $t_{\text{sub}}=0.4 \mu\text{m}$ (double Fano resonance) with $W=0.9 \mu\text{m}$, respectively. Note that both the single and multiple transparency windows are enhanced and blue shifted across a relatively large frequency range as the Fermi energy increases. This behavior can be interpreted through the resonance condition. Resonating surface

Fig. 6 Group index and imaginary part of the effective refractive index of the designed hybrid structures with $W=0.9 \mu\text{m}$ and $\mu_c=0.7 \text{ eV}$ for **a** $t_{\text{sub}}=0.8 \mu\text{m}$ and **b** $t_{\text{sub}}=0.4 \mu\text{m}$



plasmons (SPs) in graphene ribbon demand $W_{GRN} \sim N \times \frac{\lambda_{GSP}}{2}$, where N is an integer number and λ_{GSP} is the wavelength of graphene SPs. Considering the property of SPs on graphene, the resonance frequency can be derived from the quasi-static analysis [33] and expressed as

$$f_r \approx \frac{e}{c\hbar} \sqrt{\frac{\mu_c}{\eta \epsilon_{eff} W_{GRN}}} \propto \sqrt{\frac{\mu_c}{\epsilon_{eff} W_{GRN}}} \quad (2)$$

where η is a fitting parameter, c is the speed of light, and ϵ_{eff} is the effective permittivity of the media surrounding the whole structure.

Equation (2) also indicates that a larger W_{GRN} would lead to a red shift of the transparency window, which is demonstrated in Fig. 5c with $t_{sub}=0.8 \mu\text{m}$ and $\mu_c=0.7 \text{ eV}$. Besides, the influence of the surrounding media is characterized. Normally, the whole structure could be exposed in air or immersed in any liquid (or embedded in any other materials). In these cases, we assume the refractive index of the background n_{bk} in the simulation changes from 1 to 1.4 with $t_{sub}=0.8 \mu\text{m}$, $\mu_c=0.7 \text{ eV}$ and $W=0.9 \mu\text{m}$. Figure 5d demonstrates the transmittance responses of the hybrid structure with different n_{bk} . Since larger n_{bk} leads to larger ϵ_{eff} , a red shift of the transparency window is expected, which confirms Eq. (2). Therefore, the resonances and transparency windows of the hybrid structures can be tuned by merely varying the Fermi energy level of graphene with fixed geometrical parameters, and the width of the graphene ribbon and refractive index of the surrounding media provide extra degrees of freedom to further adjust the transparency windows.

The “slow wave” [34] propagation is another characteristic feature of the EIT-like system. In order to demonstrate this property in the proposed hybrid structure, we calculate the group index by utilizing the following equation:

$$n_g(\omega) = n_e(\omega) + \omega \frac{\partial n_e(\omega)}{\partial \omega} \quad (3)$$

where n_e refers to the effective refractive index, and it can be extracted from the numerical simulations of the transmission and reflection coefficients by using the well-established retrieval algorithm [35]. Figure 6a, b displays the group index and the imaginary part of the effective refractive index for $t_{sub}=0.8 \mu\text{m}$ and $t_{sub}=0.4 \mu\text{m}$, respectively, with $W=0.9 \mu\text{m}$ and $\mu_c=0.7 \text{ eV}$. It is observed that the group index for $t_{sub}=0.4 \mu\text{m}$ is much larger than that for $t_{sub}=0.8 \mu\text{m}$ within the transparency window. Inside the transparency windows for both structures, there are strong dispersions and a significantly large group index of over 55 in Fig. 6a and 175 in Fig. 6b. A group index n_g exceeding 227(336) can be observed at the transmission peak in Fig. 6a, b, implying that the electromagnetic wave passing through the same thickness of the metamaterial with a group velocity 227 (336) times slower

than that in vacuum. Because the intrinsic loss of gold is much higher than that of graphene, one would expect a larger imaginary part of effective refractive index as seen in Fig. 6. However, inside the transparency windows, the $\text{Im}(n_{eff})$ is very small, indicating that the losses are suppressed. Thus, the designed hybrid structures feature large group index and small loss within the transparency windows.

Conclusions

In conclusion, we have designed and numerically studied a graphene-based Fano metamaterials that could feature EIT-like single or double transparency windows in the THz/far-IR frequency range. For the proposed devices, the SCRR and graphene grating are treated as the “bright” mode and “quasi-dark” mode in the classic analogy of EIT, respectively. When the coupling between the graphene grating and the SCRR is enhanced, an extra transmission dip emerges in the transmission spectrum, resulting in a multi-transparency-window system. The induced EIT-like windows can be actively shifted across a large frequency range by varying the Fermi energy level of the graphene ribbon. In addition, the Fano resonances could be adjusted by modifying the width of the graphene ribbon and the surrounding media. Furthermore, the large effective group index and small imaginary part of the effective refractive index of the proposed hybrid structure indicate the capability of slowing light significantly and efficiently. The proposed structures could find numerous potential applications in tunable slow-light and sensing devices.

Acknowledgment This work is supported by research grants from the U.S. National Science Foundation under Grant Nos. ECCS-1128099, CMMI-1109971, and CMMI-1266251

Conflict of Interest The authors declare that they have no competing interests.

References

1. Miroshnichenko AE, Flach S, Kivshar YS (2010) Fano resonances in nanoscale structures. *Rev Mod Phys* 82:2257–2298
2. Chang W-S, Lassiter JB, Swanglap P, Sobhani H, Khatua S, Nordlander P, Halas NJ, Link S (2012) A plasmonic Fano switch. *Nano Lett* 12:4977–4982
3. Liu N, Hentschel M, Weiss T, Alivisatos AP, Giessen H (2011) Three-dimensional plasmon rulers. *Science* 332:1407–1410
4. Wu C, Khanikaev AB, Shvets G (2011) Broadband slow light metamaterial based on a double-continuum Fano resonance. *Phys Rev Lett* 106:107403
5. O’Hara JF, Singh R, Brener I, Smirnova E, Han J, Taylor AJ, Zhang W (2008) Thin-film sensing with planar terahertz metamaterials: sensitivity and limitations. *Opt Express* 16:1786–1795

6. Fedotov VA, Rose M, Prosvirnin SL, Papasimakis N, Zheludev NI (2007) Sharp trapped-mode resonances in planar metamaterials with a broken structural symmetry. *Phys Rev Lett* 99:147401
7. Zhang S, Genov DA, Wang Y, Liu M, Zhang X (2008) Plasmon-induced transparency in metamaterials. *Phys Rev Lett* 101:047401
8. Singh R, Rockstuhl C, Lederer F, Zhang W (2009) Coupling between a dark and a bright eigenmode in a terahertz metamaterial. *Phys Rev B* 79:085111
9. H. Raether (1988) *Surface plasmons on smooth and rough surfaces and on gratings*, Springer
10. Zharov AA, Shadrivov IV, Kivshar YS (2003) Nonlinear properties of left-handed metamaterials. *Phys Rev Lett* 91:037401
11. Khatua S, Chang W-S, Swanglap P, Olson J, Link S (2011) Active modulation of nanorod plasmons. *Nano Lett* 11:3797–3802
12. Cao T, Wei C, Simpson RE, Zhang L, Cryan MJ (2014) Fast tuning of double Fano resonance using a phase-change metamaterial under low power intensity. *Sci Rep* 4:4463
13. Novoselov KS, Geim AK, Morozov SV, Jiang D, Zhang Y, Dubonos SV, Grigorieva IV, Firsov AA (2004) Electric field effect in atomically thin carbon films. *Science* 306:666–669
14. Ju L, Geng B, Horng J, Girit C, Martin M, Hao Z, Bechtel HA, Liang X, Zettl A, Shen YR, Wang F (2011) Graphene plasmonics for tunable terahertz metamaterials. *Nat Nanotechnol* 6:630–634
15. Yan H, Low T, Zhu W, Wu Y, Freitag M, Li X, Guinea F, Avouris P, Xia F (2013) Damping pathways of mid-infrared plasmons in graphene nanostructures. *Nat Photonics* 7:394–399
16. Fang Z, Thongrattanasiri S, Schlather A, Liu Z, Ma L, Wang Y, Ajayan PM, Nordlander P, Halas NJ, García de Abajo FJ (2013) Gated tunability and hybridization of localized plasmons in nanostructured graphene. *ACS Nano* 7:2388–2395
17. Hanson GW (2008) Dyadic Green's functions and guided surface waves for a surface conductivity model of graphene. *J Appl Phys* 103:064302
18. Chuang FT, Chen PY, Cheng TC, Chien CH, Li BJ (2007) Improved field emission properties of thiolated multi-wall carbon nanotubes on a flexible carbon cloth substrate. *Nanotechnology* 18:395702
19. Hanson GW (2008) Dyadic Green's functions for an anisotropic. Non-local model of biased graphene. *IEEE Trans Antennas Propag* 56:747–757
20. Bao Q, Loh KP (2012) Graphene photonics, plasmonics, and broadband optoelectronic devices. *ACS Nano* 6:3677–3694
21. Bonaccorso F, Sun Z, Hasan T, Ferrari AC (2010) Graphene photonics and optoelectronics. *Nat Photonics* 4:611–622
22. Brar VW, Jang MS, Sherrott M, Lopez JJ, Atwater HA (2013) Highly confined tunable mid-infrared plasmonics in graphene nanoresonators. *Nano Lett* 13:2541–2547
23. Yeung KYM, Chee J, Yoon H, Song Y, Kong J, Ham D (2014) Far-infrared graphene plasmonic crystals for plasmonic band engineering. *Nano Lett* 14:2479–2484
24. Liu Y, Dong X, Chen P (2012) Biological and chemical sensors based on graphene materials. *Chem Soc Rev* 41:2283–2307
25. Gao W, Shu J, Qiu C, Xu Q (2012) Excitation of plasmonic waves in graphene by guided-mode resonances. *ACS Nano* 6:7806–7813
26. Chen Z, Chen J, Wu Z, Hu W, Zhang X, Lu Y (2014) Tunable Fano resonance in hybrid graphene-metal gratings. *Appl Phys Lett* 104:161114
27. M. Amin, M. Farhat, and H. Bağcı (2013) A dynamically reconfigurable Fano metamaterial through graphene tuning for switching and sensing applications, *Scientific Reports*. 3
28. Ordal MA, Long LL, Bell RJ, Bell SE, Bell RR, Alexander RW, Ward CA (1983) Optical properties of the metals Al Co, Cu, Au, Fe, Pb, Ni, Pd, Pt, Ag, Ti, and W in the infrared and far infrared. *Appl Optics* 22:1099–1119
29. Gusynin VP, Sharapov SG, Carbotte JP (2007) Magneto-optical conductivity in graphene. *J Phys: Condens Matter* 19:026222
30. Hanson GW (2008) Quasi-transverse electromagnetic modes supported by a graphene parallel-plate waveguide. *J Appl Phys* 104:084314
31. Vakil A, Engheta N (2011) Transformation optics using graphene. *Science* 332:1291–1294
32. Tassin P, Zhang L, Koschny T, Economou EN, Soukoulis CM (2009) Low-loss metamaterials based on classical electromagnetically induced transparency. *Phys Rev Lett* 102:053901
33. Nikitin AY, Guinea F, Garcia-Vidal FJ, Martin-Moreno L (2012) Surface plasmon enhanced absorption and suppressed transmission in periodic arrays of graphene ribbons. *Phys Rev B* 85:081405
34. Zhang L, Tassin P, Koschny T, Kurter C, Anlage SM, Soukoulis CM (2010) Large group delay in a microwave metamaterial analog of electromagnetically induced transparency. *Appl Phys Lett* 97:241904
35. Smith DR, Vier DC, Koschny T, Soukoulis CM (2005) Electromagnetic parameter retrieval from inhomogeneous metamaterials. *Phys Rev E* 71:036617